NATIONAL ADVISORY COMMITTEE FOR AERONAUTICS

REPORT No. 273

WIND TUNNEL TESTS ON AUTOROTATION AND THE "FLAT SPIN"

By MONTGOMERY KNIGHT

UNITED STATES
GOVERNMENT PRINTING OFFICE
WASHINGTON
1927

AERONAUTICAL SYMBOLS

1. FUNDAMENTAL AND DERIVED UNITS

	Symbol	Metric		English	
		Unit	Symbol	Unit	Symbol
Length	l	meter	m	foot (or mile)	ft. (or mi.)
Time	t	second	sec	second (or hour)	sec. (or hr.)
Force	F	weight of one kilogram	kg	weight of one pound	lb.
Power	P	kg/m/sec		horsepower	HP.
Speed		km/hr		mi./hr	M. P. H.
		m/sec		ft./sec	f. p. s.

2. GENERAL SYMBOLS, ETC.

W, Weight, $=mg$

g, Standard acceleration of gravity $=9.80665$ m/sec.^{2} $=32.1740$ ft./sec.^{2}

m, Mass, $=\frac{W}{g}$

ρ, Density (mass per unit volume).

Standard density of dry air, 0.12497 (kg-m^{-4} sec.^{2}) at 15° C and 760 mm $=0.002378$ (lb.-ft.$^{-4}$ sec.^{2}).

Specific weight of "standard" air, 1.2255 kg/m^3 $=0.07651$ lb./ft.^{3}

mk^2, Moment of inertia (indicate axis of the radius of gyration, k, by proper subscript).

S, Area.

S_w, Wing area, etc.

G, Gap.

b, Span.

c, Chord length.

b/c, Aspect ratio.

f, Distance from $c.\ g.$ to elevator hinge.

μ, Coefficient of viscosity.

3. AERODYNAMICAL SYMBOLS

V, True air speed.

q, Dynamic (or impact) pressure $=\frac{1}{2}\rho V^2$

L, Lift, absolute coefficient $C_L=\frac{L}{qS}$

D, Drag, absolute coefficient $C_D=\frac{D}{qS}$

C, Cross-wind force, absolute coefficient $C_C=\frac{C}{qS}$

R, Resultant force. (Note that these coefficients are twice as large as the old coefficients L_C, D_C.)

i_w Angle of setting of wings (relative to thrust line).

i_t, Angle of stabilizer setting with reference to thrust line.

γ, Dihedral angle.

$\rho\frac{Vl}{\mu}$, Reynolds Number, where l is a linear dimension.

e. g., for a model airfoil 3 in. chord, 100 mi./hr. normal pressure, 0° C: 255,000 and at 15° C., 230,000;

or for a model of 10 cm chord 40 m/sec, corresponding numbers are 299,000 and 270,000.

C_p, Center of pressure coefficient (ratio of distance of $C.\ P.$ from leading edge to chord length).

β, Angle of stabilizer setting with reference to lower wing, $=(i_t-i_w)$.

α, Angle of attack.

ϵ, Angle of downwash.

REPORT No. 273

WIND TUNNEL TESTS ON AUTOROTATION AND THE "FLAT SPIN"

By MONTGOMERY KNIGHT
Langley Memorial Aeronautical Laboratory

53898—27——1

NATIONAL ADVISORY COMMITTEE FOR AERONAUTICS

NAVY BUILDING, WASHINGTON, D. C.

[An independent Government establishment, created by act of Congress approved March 3, 1915, for the supervision and direction of the scientific study of the problems of flight. It consists of 12 members who are appointed by the President, all of whom serve as such without compensation.]

JOSEPH S. AMES, Ph. D., *Chairman*,
Provost, Johns Hopkins University, Baltimore, Md.
DAVID W. TAYLOR, D. Eng., *Vice Chairman*,
Washington, D. C.
GEORGE K. BURGESS, Sc. D.,
Director, Bureau of Standards, Washington, D. C.
WILLIAM F. DURAND, Ph. D.,
Professor Emeritus of Mechanical Engineering, Stanford University, Calif.
WILLIAM E. GILLMORE, Brigadier General, United States Army,
Chief, Matériel Division, Air Corps, Dayton, Ohio.
EMORY S. LAND, Captain, United States Navy,
Assistant Chief, Bureau of Aeronautics, Navy Department, Washington, D. C.
CHARLES F. MARVIN, M. E.,
Chief, United States Weather Bureau, Washington, D. C.
WILLIAM A. MOFFETT, Rear Admiral, United States Navy,
Chief, Bureau of Aeronautics, Navy Department, Washington, D. C.
MASON M. PATRICK, Major General, United States Army,
Chief of Air Corps, War Department, Washington, D. C.
S. W. STRATTON, Sc. D.,
President, Massachusetts Institute of Technology, Cambridge, Mass.
ORVILLE WRIGHT, B. S.,
Dayton, Ohio.
———— ————,
Smithsonian Institution, Washington, D. C.

GEORGE W. LEWIS, *Director of Aeronautical Research.*
JOHN F. VICTORY, *Secretary.*

EXECUTIVE COMMITTEE

JOSEPH S. AMES, *Chairman.*
DAVID W. TAYLOR, *Vice Chairman.*

GEORGE K. BURGESS.	WILLIAM A. MOFFETT.
WILLIAM E. GILLMORE.	MASON M. PATRICK.
EMORY S. LAND.	S. W. STRATTON.
CHARLES F. MARVIN.	ORVILLE WRIGHT.

JOHN F. VICTORY, *Secretary.*

REPORT No. 273

WIND TUNNEL TESTS ON AUTOROTATION AND THE "FLAT SPIN"

By Montgomery Knight

SUMMARY

The following report deals with the autorotational characteristics of certain differing wing systems as determined from wind tunnel tests made at the Langley Memorial Aeronautical Laboratory. The investigation was confined to autorotation about a fixed axis in the plane of symmetry and parallel to the wind direction. Analysis of the tests leads to the following conclusions:

Autorotation below 30° angle of attack is governed chiefly by wing profile, and above that angle by wing arrangement.

The strip method of autorotation analysis gives uncertain results between maximum C_L and 35°.

The polar curve of a wing system, and to a lower degree of accuracy the polar of a complete airplane model are sufficient for direct determination of the limits of rotary instability, subject to strip method limitations.

The results of the investigation indicate that in free flight a monoplane is incapable of flat spinning, whereas an unstaggered biplane has inherent flat-spinning tendencies.

The difficulty of maintaining equilibrium in stalled flight is due primarily to rotary instability, a rapid change from stability to instability occurring as the angle of maximum lift is exceeded.

INTRODUCTION

Autorotation may be explained by a consideration of the torques brought into play by the rotation of a wing or combination of wings about an axis in the plane of symmetry and parallel to the wind direction. This phenomenon is recognized as a vital factor in the "spin" of an airplane.

The so-called "flat spin" may be defined as a spin in which the longitudinal axis of the airplane is more nearly horizontal than vertical in contradistinction to the "normal spin" in which the reverse is true. The flat spin is a characteristic of certain unstaggered biplanes, notably the British B. A. T. *Bantam* and Short *Springbok*, and the American Boeing *NB–1*. This type of spin is considered dangerous owing to the difficulty of returning to normal flight, and means of insuring against its occurrence are being sought.

Autorotation has been studied for several years with the aid of wind tunnel rotational experiments and mathematical analyses based on force tests. Spinning tests of airplanes in free flight have also been made, and these have been supplemented by tests upon light models dropped from a height.

The present investigation was instituted for a further study of autorotation with emphasis laid upon the flat spin. Three airfoils of widely differing characteristics were tested as monoplanes, and tests were also made on an unstaggered biplane cell.

The experiments, which consisted of both force and rotation tests from zero lift to 90° angle of attack, were conducted in the 5-foot, circular-throat, atmospheric wind tunnel (Reference 1) of the Langley Memorial Aeronautical Laboratory.

In this report three terms are used with reference to rotation about a fixed axis in the plane of symmetry and parallel to the wind direction. They are defined as follows:

1. "Stable autorotation" signifies a state of equilibrium in autorotation to which the model returns whenever disturbed therefrom.

2. "Unstable autorotation" signifies a state of equilibrium in autorotation such that a small disturbance aiding the rotation causes stable autorotation, while an opposing disturbance brings the model to rest.

3. "Rotary instability" signifies a state of equilibrium in rectilinear motion such that a small rotary disturbance causes stable autorotation.

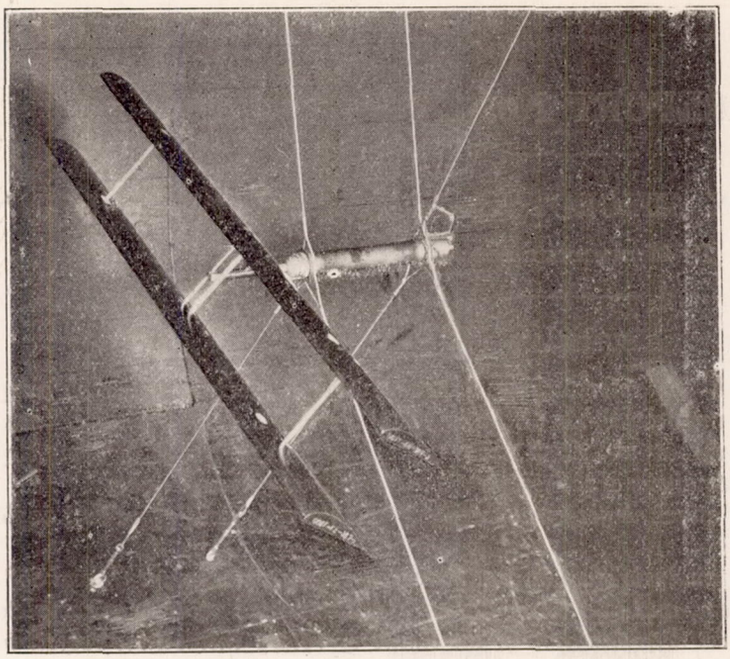

FIG. 1.—Biplane mounted on autorotation apparatus

APPARATUS AND TESTS

Three airfoil profiles were used in the tests. These were Göttingen 387–FB (flat bottom), R. A. F. 15, and N. A. C. A.–M1. Rectangular wings, 5 by 30 inches in plan, having these profiles were tested as monoplanes. An unstaggered biplane cell of Göttingen 387–FB profile was also tested.

The autorotation apparatus, illustrated in Figures 1 and 2, consisted of a barrel containing ball bearings supporting a shaft upon which the models were mounted as shown. A simple screw adjustment permitted locking of the model at any desired angle of attack. A reduction gear and electrical contact at the down-wind end of the barrel operated a light outside the tunnel for determining rates of rotation.

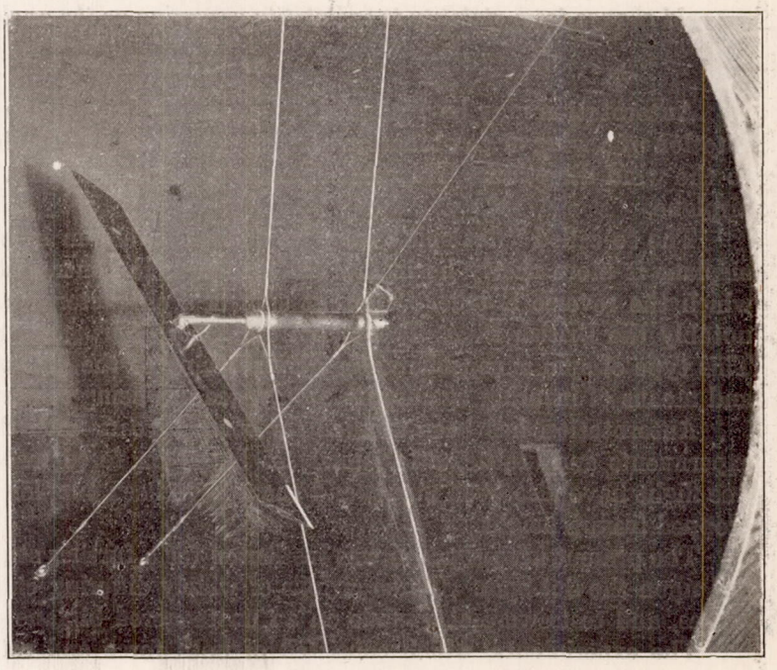

FIG. 2.—Monoplane mounted on autorotation apparatus

The average rates of rotation in opposite directions for a given mean angle of attack α_m gave the results presented below. The limits of rotary instability were obtained merely by noting the angles of attack between which stable autorotation was induced when the model was disturbed slightly from rest.

The force tests were made on the regular wire balance of the tunnel (Reference 1). Lift and drag were measured from approximately zero lift to 90° angle of attack. The biplane drag coefficients are corrected for strut drag.

All tests were run at a dynamic pressure of 20.2 kg/m^2 (4.13 lb./sq. ft.), representing an average air speed of 18 m/s (40.3 M. P. H.), and an average Reynolds Number of 153,000.

Rates of rotation were checked to within ± 1 per cent. Limits of rotary instability may be relied upon to $\pm 1°$ and angles of attack to $\pm 0.1°$. The lift and drag data are accurate to ± 1.5 per cent. The dynamic pressure showed a maximum variation of ± 0.5 per cent.

RESULTS

TESTS

The results of the autorotation tests may be found in Tables I–IV and Figures 3–7, inclusive. Rates of stable autorotation are plotted against mean angles of attack in the curves. Rates of rotation are expressed nondimensionally in terms of the linear and angular velocities u and p, respectively, as

$$\tan \Phi = \frac{pb}{2u}$$

where b = span. This expression is merely the ratio of the wing tip speed to forward speed, and is analogous to the tangent of the effective helix angle of a propeller tip.

Force test results are given in Tables V–VIII and Figures 8–12. Lift and drag are plotted against one another in the polar curves, the customary absolute coefficients being used.

$$C_L = \frac{L}{qS}$$

$$C_D = \frac{D}{qS}$$

where L and D are the lift and drag, respectively, S the area, and q the test dynamic pressure ($q = \frac{1}{2}\rho V^2$, where ρ = density, V = air speed) all in consistent units.

No corrections are made for tunnel wall effects, and hence these results are not "free air" data for the models tested.

AUTOROTATION CALCULATIONS

The strip method as applied to the analysis of autorotation consists in treating individual wing elements (parallel to the plane of symmetry) separately, and computing the torque due to each on the basis of their helical motions. Summation then gives the resultant torque for the entire wing which must be zero for the condition of stable autorotation. Ordinary force tests carried to high angles of attack (assuming uniform distribution of resultant force across the span) furnish the data for these computations. In the present work no account is taken of the modification of force distribution by the tip form of the model, by centrifugal force and scale effect due to rotation, or by the tunnel walls. This is the usual practice, but as demonstrated later, these factors are by no means negligible under certain conditions.

The customary analysis, first made by Glauert, utilizes the curves of lift and drag against angle of attack. (References 2, 3, 4, and 5.) However, the work done at this laboratory has shown that the polar curve furnishes a simpler basis for the analysis. In addition, the polar itself is a means for the direct determination of the limits of rotary instability, subject to the same limitations as the strip method.

Expressions for torque and force coefficients in rotation and the corresponding criterion for rotary instability are derived on the basis of resultant force in the Appendix. The criterion is

$$\frac{d(C_R)}{d\alpha} < 0$$

where C_R is the absolute coefficient of resultant force, and α, the angle of attack of the wing. This criterion is an approximation but, for all practical purposes, it gives the same results as

Glauert's exact expression. (See Appendix.) Both criteria are subject to strip method limitations.

The new criterion makes the polar a sufficient means of determining the ranges of rotary instability, since the relation signifies a decreasing resultant force with increasing angle of attack. For this purpose it is essential that the true polar (equal ordinates and abscissas) be used. The limits of instability may be found merely by noting the angles of attack at which

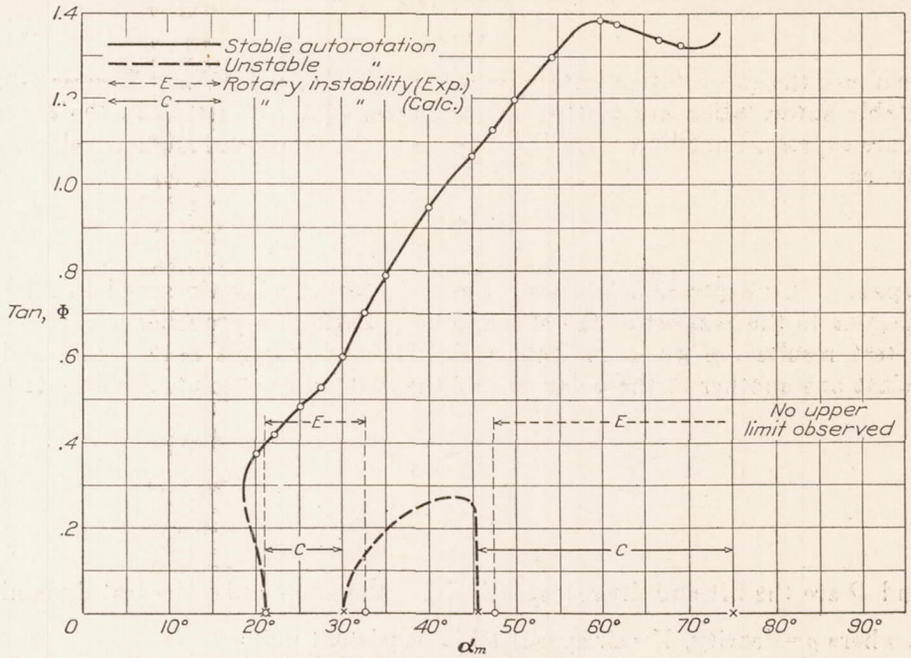

FIG. 3.—Autorotation test on Göttingen 387–FB biplane (5 by 30 inches), $G/c=1$, stagger=0, $q=20.2$ kg/m², Reynolds No. =155,000

the polar curve is perpendicular to a line drawn from the origin. The relative degree of stability or instability at various angles (α_m) is indicated roughly by $\cos \alpha_m \frac{dC_R}{d\alpha}$. (See fig. 15.)

The calculated ranges of rotary instability are included in Figures 3–6 and 8–11 for comparison with the experimental results.

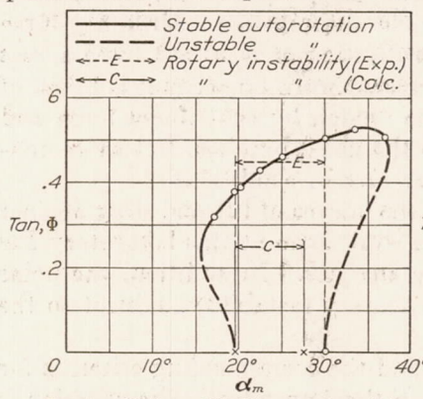

FIG. 4.—Göttingen 387–FB monoplane (5 by 30 inches), $q=20.2$ kg/m², Reynolds No. = 153,000

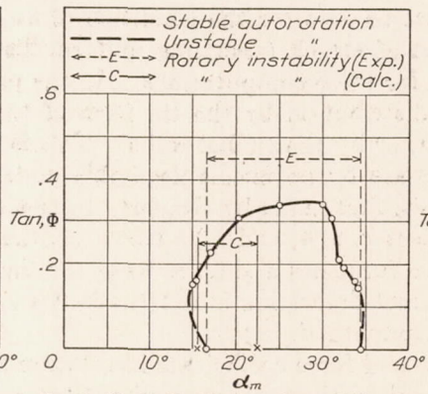

FIG. 5.—R. A. F. 15 monoplane (5 by 30 inches), $q=20.2$ kg/m², Reynolds No. =152,000

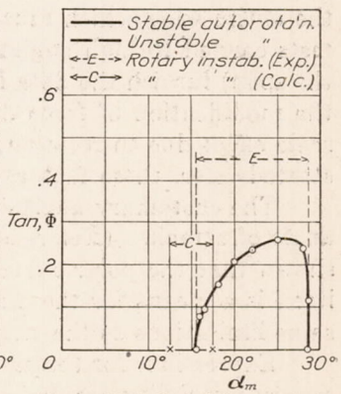

FIG. 6.—N. A. C. A. M1 monoplane (5 by 30 inches), $q=20.2$ kg/m², Reynolds No. = 153,000

DISCUSSION OF RESULTS

AUTOROTATION TESTS

The test results shown in Figure 7 furnish a striking demonstration of the possible variation in autorotational characteristics of common types of airfoils and airfoil combinations. An outstanding feature is the wide difference, both in range and in magnitude, between monoplane and biplane results, illustrating the already recognized effect of multiplane interference.

The differing rates and ranges of autorotation up to 45° furnish a means of comparing the effects of different airfoil profiles upon autorotation.

Another and unanticipated feature is the well-defined autorotation of the symmetrical M1 airfoil, for which strip method calculations predicted but a slight degree of instability.

The experimental autorotation curves are merely interpolated for unstable autorotation (shown by dotted lines in Figures 3, 4, and 5) since the apparatus did not permit of obtaining these values experimentally. In Figure 3 is included also a calculated curve of the values of tan Φ at which unstable autorotation occurs for the biplane. These additions are intended only as a rough indication of existing conditions.

FORCE TESTS AND AUTOROTATION CALCULATIONS

The polar diagrams in Figure 12 afford another illustration of the marked difference between the characteristics of the monoplane and the unstaggered biplane. This difference has previously been attributed to the shielding of the upper wing of a biplane by the lower (References 6

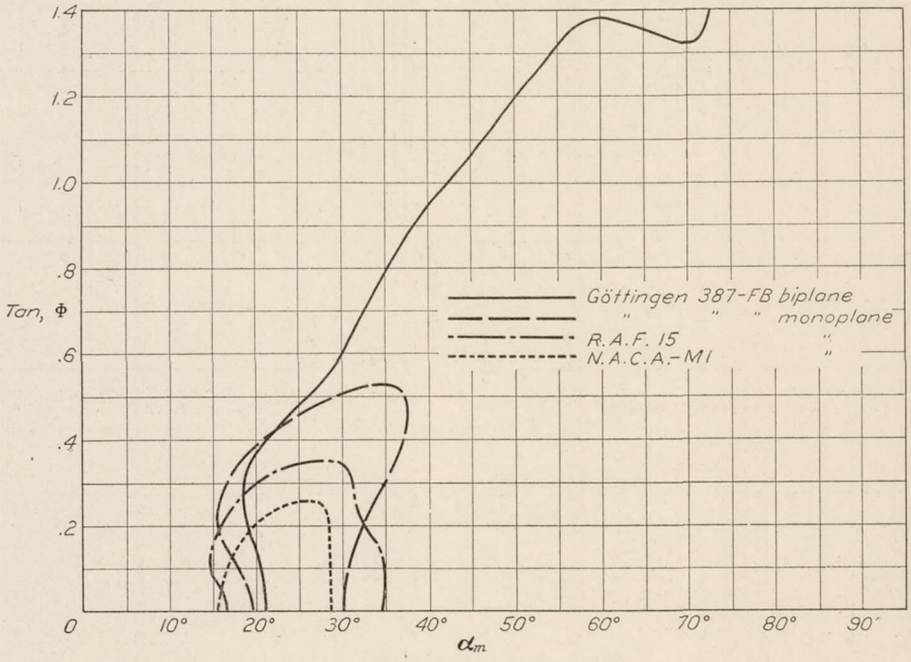

FIG. 7.—Autorotation tests on four models

and 7), and recent biplane pressure distribution experiments carried to 90° angle of attack (conducted at this laboratory), proved this fact conclusively. Positive stagger or upper wing overhang may be expected to reduce biplane autorotational tendencies by reducing this shielding, thereby approaching the monoplane condition. (Reference 8.) The same may be said for an increase in gap, except that for practical gap-chord ratios the reduction in shielding due to gap increase will probably be small compared with that for stagger increase, or for overhang. However, it was not possible at the time of test to include an investigation of the effects of stagger, overhang, and gap throughout the first quadrant, and very little data of this nature for angles of attack above 30° has been made available elsewhere up to this time.

In Figures 8–11 the calculated and experimental ranges of rotary instability are shown to demonstrate the use of the polar as a criterion. These curves show that, with the exception of the M1 wing, the lower limits of instability are in good agreement and for each wing are practically at the point of maximum C_L. None of the monoplanes show, either by experiment or calculation, any definite tendency to rotate above 35°, while the biplane has distinct autorotational tendencies in the region above 45°.

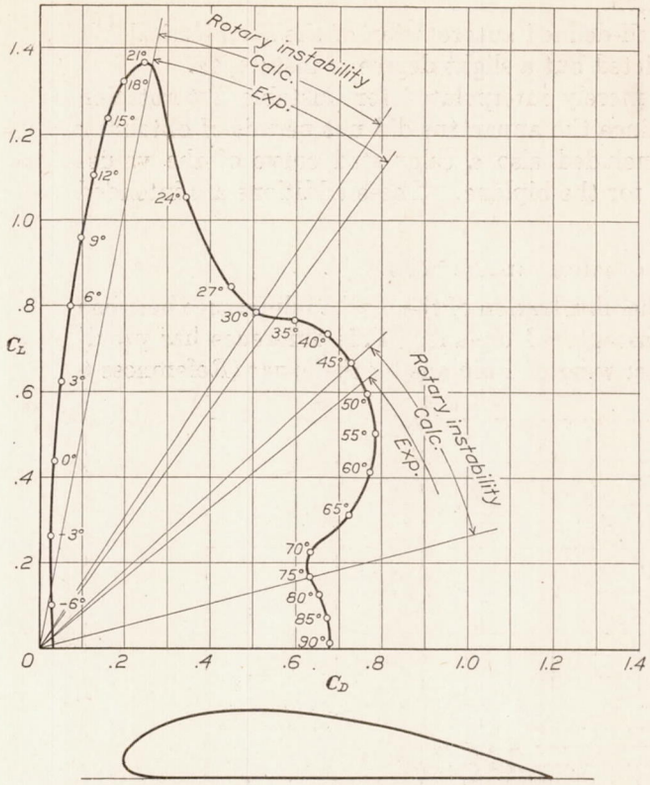

FIG. 8.—Force test on Göttingen 387–FB biplane (5 by 30 inches) G/c=1, stagger=0, q=20.2 kg/m², Reynolds No.=156,000

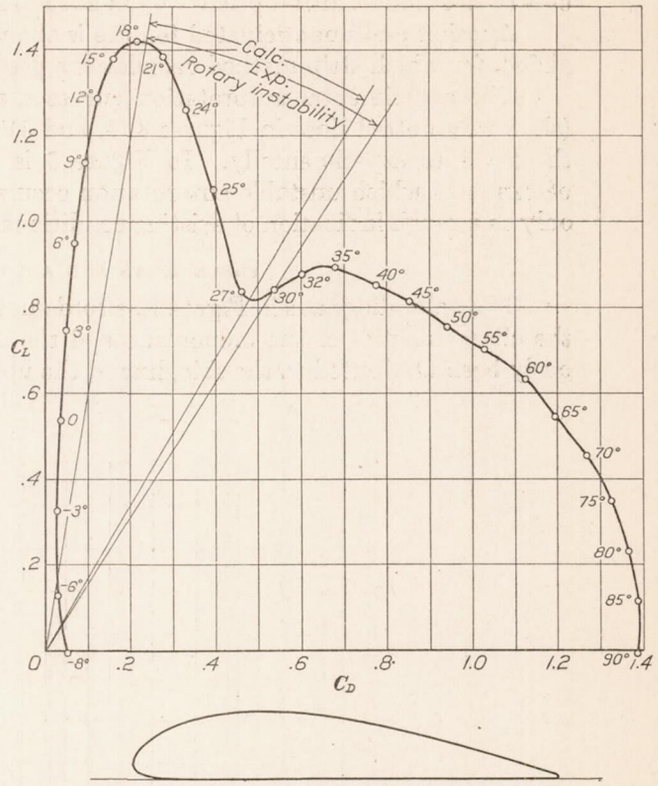

FIG. 9.—Force test on Göttingen 387–FB monoplane (5 by 30 inches), q=20.2 kg/m², Reynolds No.=155,000

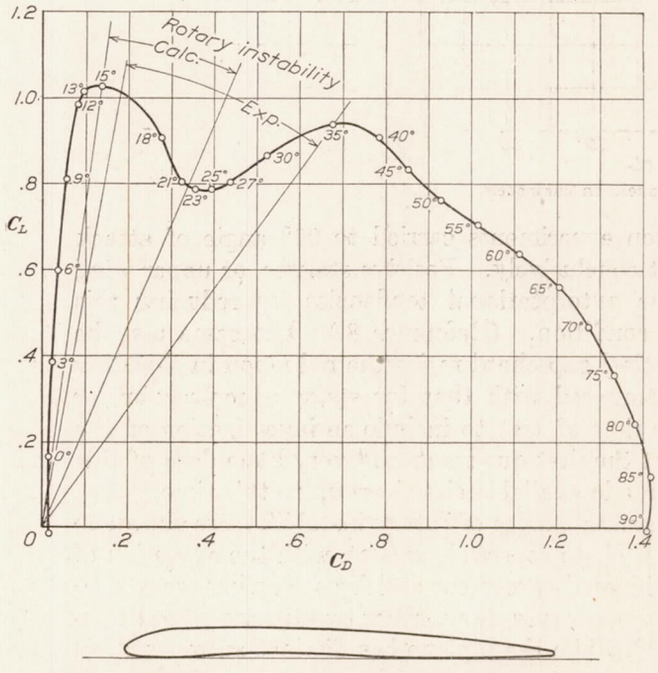

FIG. 10.—Force test on R. A. F. 15 monoplane (5 by 30 inches), q=20.2 kg/m², Reynolds No.=155,000

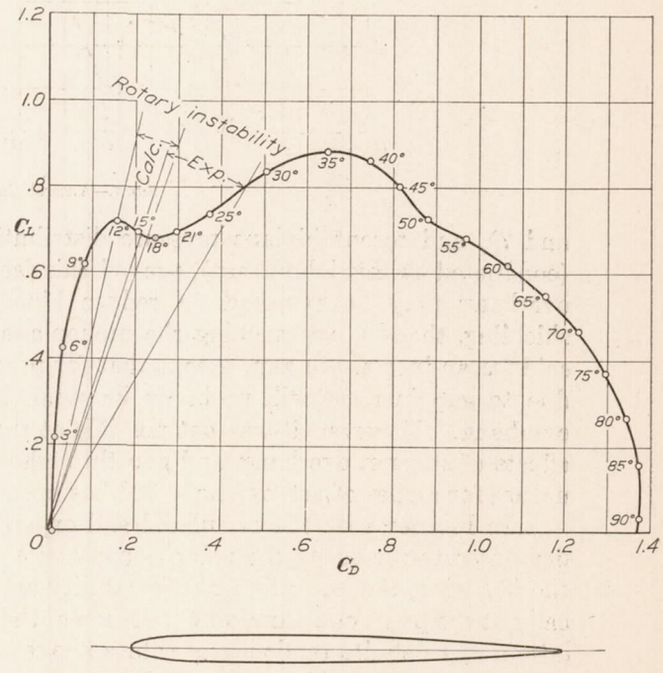

FIG. 11.—Force test on N. A. C. A.=M1 monoplane (5 by 30 inches), q=20.2 kg/m², Reynolds No.=156,000

Figures 10 and 11 show that the accuracy of the strip method is to be questioned between the angles of maximum C_L and 35°, though it may be relied on reasonably well beyond these limits. Doubtless the discrepancies may be attributed largely to the basic assumption of uniform force distribution across the span.

The very apparent similarity of the monoplane polars from 30° to 90°, and the wide differences between monoplane and biplane in Figure 12, indicate that wing arrangement and not wing profile is the controlling factor over this range.

The radial lines drawn in Figure 12 together with the points shown on the curves indicate the relative positions of the normal to the chord and the resultant force vectors for 30°, 45°, and 90° angle of attack. Figure 17 shows this relationship more completely, and it is evident that between 30° and 90° departure of the resultant force vector from the normal to the chord is less than ±3°, for any of the models tested.

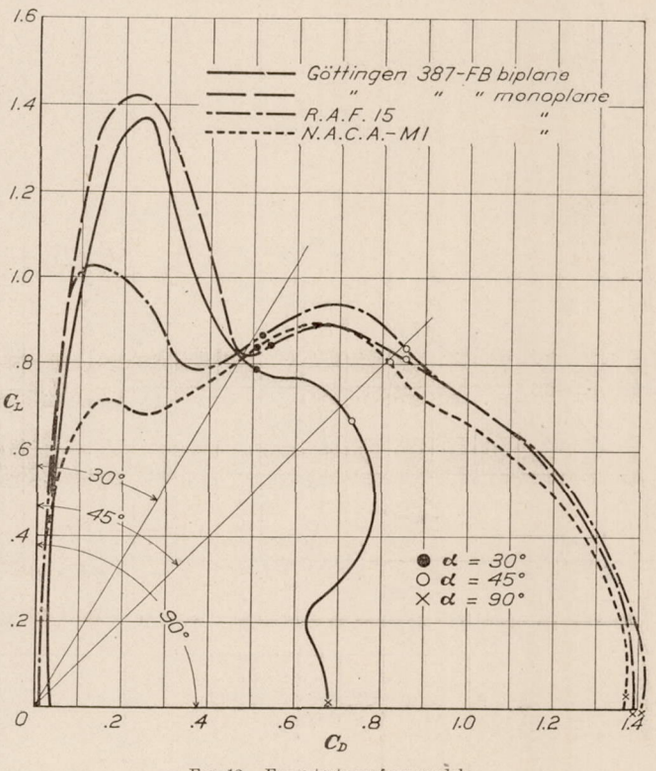

FIG. 12.—Force tests on four models

Figures 13 and 14 are included in this report to demonstrate the feasibility of using the first quadrant polar of complete airplane models for determining roughly their limits of rotary instability. Figure 13 is taken from force tests made at the Washington Navy Yard upon a 1/16 scale model of the Boeing NB–1 seaplane. (Reference 9.) Similar results for a 1/24 scale model of the Douglas XO–2 landplane are given in Figure 14, as obtained from tests recently made at this laboratory at the request of the Army Air Corps. Calculated ranges of rotary instability are shown on these curves. Experimental ranges for the XO–2 are given in Figure 14.

The criterion for rotary instability is developed from the strip method analysis of wing systems only. Therefore the presence in the complete model polars of the forces upon body, tail, and landing gear may be expected to introduce errors in determining the limits of rotary instability. However, in spite of these spurious effects, flat-spinning tendencies are distinctly indicated for the models in Figures 13 and 14, and in the latter figure the calculated ranges of instability are in fair agreement with experiment.

In Figure 15 are shown curves of the complete criterion for rotary instability, $\frac{d(C_A)}{d\alpha}$, against angle of attack. (See Appendix for derivation.) This criterion indicates not only the state of equilibrium, but also the degree of stability or instability. The points shown are values of $\cos \alpha_m \frac{d(C_R)}{d\alpha}$ and are included to show that the simpler expression may be used with good accuracy. The following deductions may be made from these curves:

Maximum damping (stable) tendencies occur at or near zero angle of attack and are of practically the same magnitude for all the models tested.

Maximum autorotational (unstable) tendencies occur in each case just beyond maximum lift, and vary widely in magnitude for the different models.

Beyond 35° the characteristics of the monoplanes are practically identical, with small stable tendencies between 45° and 75°, and practically neutral equilibrium at 45° and between 75° and 90°.

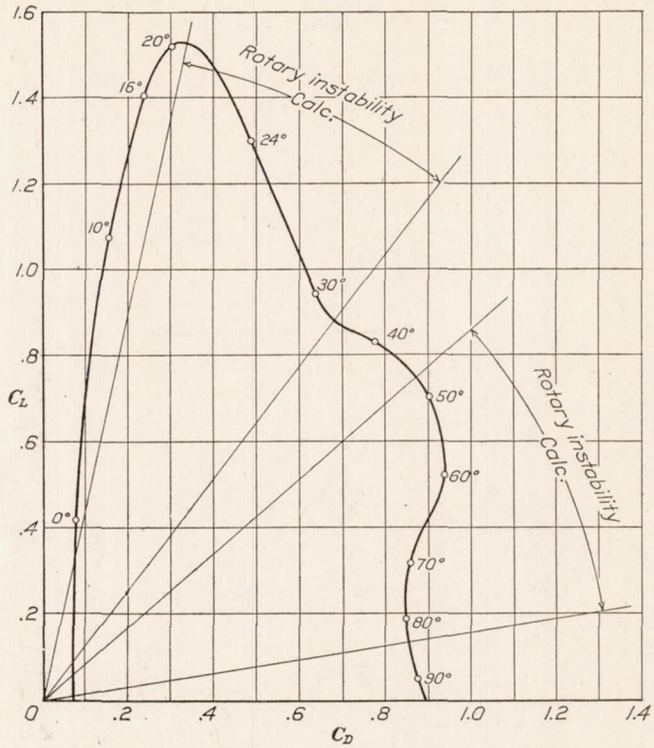

FIG. 13.—Force test on Boeing NB-1 seaplane, 1/16 scale model. V=40 M. P. H.

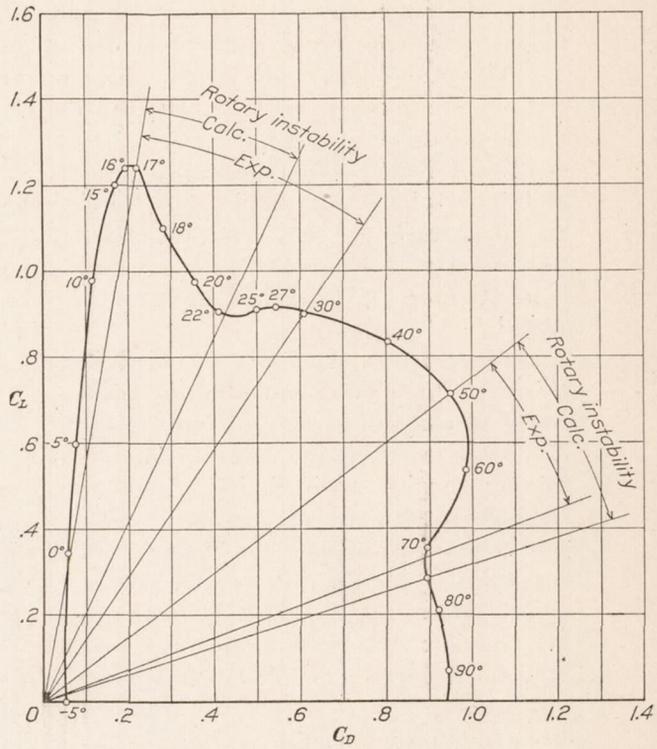

FIG. 14.—Force test on Douglas XO-2 airplane, 1/24 scale model. q=55.5 kg/m²

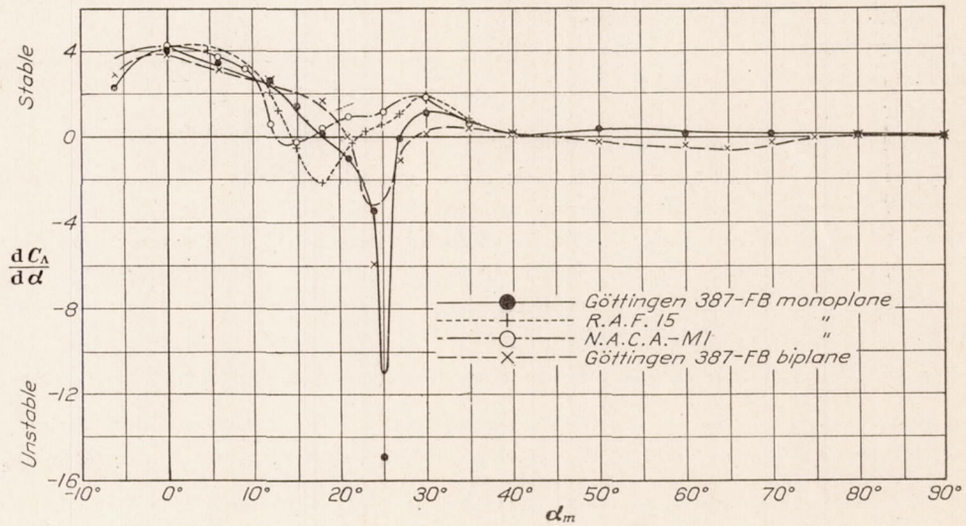

FIG. 15.—Rotary stability curves, $\frac{dC_A}{d\alpha}$

Beyond 45° the biplane shows instability, and neutral equilibrium between 75° and 90°.

As the angle of maximum lift is exceeded, strip method and test results begin to diverge, agreement being reached again at 35°. Due to this divergence no attempt can safely be made to interpret the curves between these limits.

By far the most important deduction to be made relates to stalled flight. The curves show that in the vicinity of maximum lift there is for each model a rapid change from rotary stability to instability. This means that the orthodox airplane in flight suddenly becomes laterally unstable as maximum lift is passed, and if small rotary disturbances are not promptly corrected for by ailerons and rudder, the rapidly increasing autorotational forces may become large enough to overcome the control forces, and a spin ensues.

For greater safety in flight every effort should be made in the direction of maintaining rotary stability and improving lateral control above the stall. Especially should rotary instability be an immediate object of investigation in wind tunnel and free flight research.

CONCLUSIONS

Although this investigation is far from being exhaustive, the following general conclusions may safely be drawn from it:

1. Autorotation below 30° angle of attack is governed largely by wing profile, and above that angle by wing arrangement.
2. The strip method of analysis furnishes a criterion for rotary instability which is in good agreement with experiment above 35° and also in the vicinity of maximum C_L.
3. Strip method results are to be questioned between maximum C_L and 35°, and this fact calls for further investigation of that region.
4. The polar curve of a wing system furnishes means for the direct determination of the limits of rotary instability and, for a rough indication, the polar of a complete airplane model may be used similarly, subject in both cases to strip method limitations.

The following statements relative to the airplane in free flight may now be made with reasonable assurance:

1. An airplane with a monoplane wing is not capable of flat spinning.
2. An airplane with unstaggered biplane wings has inherent flat-spinning tendencies.
3. Positive stagger or upper wing overhang may be expected to reduce flat-spinning tendencies.
4. The difficulty of maintaining equilibrium in stalled flight is due primarily to rotary instability, a rapid change from stability to instability occurring as the angle of maximum lift is exceeded.

LANGLEY MEMORIAL AERONAUTICAL LABORATORY,
NATIONAL ADVISORY COMMITTEE FOR AERONAUTICS,
LANGLEY FIELD, VA., *April 21, 1927.*

REFERENCES AND BIBLIOGRAPHY

1. Reid, Elliott G. Standardization Tests of N. A. C. A. No. 1 Wind Tunnel. N. A. C. A. Technical Report No. 195. 1924.

2. Glauert, H. The Rotation of an Aerofoil about a Fixed Axis. B. A. C. A. Reports and Memoranda No. 595. March, 1919.

3. Glauert, H. The Investigation of the Spin of an Aeroplane. B. A. C. A. Reports and Memoranda No. 618. June, 1919.

4. Bradfield, F. B. Lateral Control of Bristol Fighter at Low Speeds. Measurement of Rolling and Yawing Moments of Model Wings, Due to Rolling. B. A. C. A. Reports and Memoranda No. 787. January, 1921.

5. Anderlik, E. Experiments on Autorotation. N. A. C. A. Technical Memorandum No. 380. 1926. (Translated from "Zeitschrift für Flugtechnik und Motorluftschiffahrt," August 28, 1926.)

6. Bradfield, F. B., and Simmonds, O. E. Rolling and Yawing Moments Due to Roll of Model Avro Wings with Standard and Interplane Ailerons, and Rudder Moments for Standard and Special Large Rudder. B. A. C. A. Reports and Memoranda No. 848. November, 1922.

7. Townend, H. C. H., and Kirkup, T. A. Some Experiments on a Model of a B. A. T. Bantam Aeroplane with Special Reference to Spinning Accidents. B. A. C. A. Reports and Memoranda No. 976. November, 1925.

8. Irving, H. B., and Batson, A. S. Preliminary Note on the Effect of Stagger and Decalage on the Autorotation of a R. A. F. 15 Biplane. B. A. C. A. Reports and Memoranda No. 733. September, 1920.

9. Aeronautics Staff. Air Force and Moment for NB–1 Airplane. Construction Department, Washington Navy Yard. Aeronautical Report No. 282. June, 1925.

10. Thomson, G. P. Calculations on the Spinning of an Aeroplane. B. A. C. A. Reports and Memoranda No. 211. November, 1915.

11. Lindemann, F. A., Glauert, H., and Harris, R. G. The Experimental and Mathematical Investigation of Spinning. B. A. C. A. Reports and Memoranda No. 411. March, 1918.

12. Relf, E. F., and Lavender, T. The Autorotation of Stalled Aerofoils and Its Relation to the Spinning Speed of Aeroplanes. B. A. C. A. Reports and Memoranda No. 549. October, 1918.

13. Relf, E. F., and Lavender, T. A Continuous Rotation Balance for the Measurement of L_p at Small Rates of Roll. B. A. C. A. Reports and Memoranda No. 828. August, 1922.

14. Bradfield, F. B., and Coombes, L. P. Autorotation Measurements on a Model Aeroplane with Zero Stagger. B. A. C. A. Reports and Memoranda No. 975. April, 1925.

15. Ofstie, Ralph A. The Flat Spin of the Boeing N. B. Training Airplane. Bureau of Aeronautics, Navy Department. Technical Note No. 164. May, 1926.

16. Lachmann, G. Stall-Proof Airplanes. N. A. C. A. Technical Memorandum No. 393. 1927. (Translation from the Yearbook of the "Wissenschaftlichen Gesellschaft für Luftfahrt," 1925.)

17. Bryant, L. W., and Gates, S. B. The Spinning of Aeroplanes. "The Journal of the Royal Aeronautical Society." July, 1927.

APPENDIX

STRIP METHOD ANALYSIS

Following is the strip method derivation of the expressions for torque and force coefficients in rotation, and also the development of a criterion for rotary instability.

The symbols used are illustrated in Figure 16. C_R is the resultant force coefficient (absolute) for the angle of attack α, while C_Δ and C_Δ are its components, respectively, along and normal to the axis of rotation. The angle of the wing chord to this axis is α_m. The effective wind velocity V_E is the vector sum of the velocity V along the axis and the tangential velocity V_R. The wing chord and span are represented by c and b, respectively, and, in this derivation, c is a constant.

Therefore the torque increment due to a given wing element of width Δy at a distance y from the axis of rotation may be written

$$\Delta\Lambda = C_\Lambda q' yc\,(\Delta y) \tag{1}$$

where

$$q' = \frac{1}{2}\rho V_E^2$$

$$= \frac{1}{2}\rho\,(V \sec \Delta\alpha)^2$$

$$= q\,(\sec^2 \Delta\alpha) \tag{2}$$

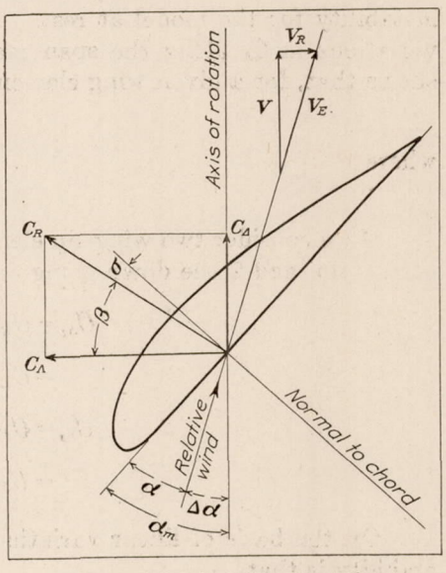

FIG. 16.—Wing element in autorotation

$\Delta\alpha$ being the algebraic sum of the angle of attack of the element in question and α_m. The total torque for the wing is therefore

$$\Lambda = qc\int_{-b/2}^{b/2} C_\Lambda y\,(\sec^2 \Delta\alpha)\,dy \tag{3}$$

and reduced to nondimensional coefficient form

$$C_\lambda = \frac{\Lambda}{qbS} = \frac{\Lambda}{qb^2c}$$

$$= \frac{1}{b^2}\int_{-b/2}^{b/2} C_\Lambda y\,(\sec^2 \Delta\alpha)\,dy \tag{4}$$

where C_λ is the coefficient of autorotational moment. The lift coefficient (force normal to axis) is

$$C_L = \frac{1}{b^2}\int_{-b/2}^{b/2} C_\Lambda\,(\sec^2 \Delta\alpha)\,dy \tag{4a}$$

The corresponding equation for moment about an axis in the plane of symmetry and normal to that of autorotation is similarly

$$C_\delta = \frac{1}{b^2}\int_{-b/2}^{b/2} C_\Delta y \,(\sec^2 \Delta\alpha)\, dy \tag{4b}$$

while the drag coefficient in rotation is

$$C_D = \frac{1}{b^2}\int_{-b/2}^{b/2} C_\Delta \,(\sec^2 \Delta\alpha)\, dy \tag{4c}$$

If we now consider very small angular velocities we may determine the criterion of rotary instability for the model at rest. The angular velocity is to be taken sufficiently small that variations in C_Δ along the span may be considered linear. For this condition equation (1) shows that, for a given wing element, the increment of torque

$$\Delta\Lambda = KC_\Delta$$

where

$$K = q' yc\,(\Delta y).$$

If we consider two wing-tip elements (1, 2) such that 1 is on the up-going or small-angle-of-attack tip, and 2 the down-going or large-angle tip, we have from Figure 16

$$C_{\Delta_1} = C_{R_1}\cos\beta_1 = C_{R_1}\cos(\alpha_m - \sigma_1)$$

$$= C_{R_1}(\cos\alpha_m\cos\sigma_1 + \sin\alpha_m\sin\sigma_1)$$

$$C_{\Delta_2} = C_{R_2}\cos\beta_2 = C_{R_2}\cos(\alpha_m - \sigma_2)$$

$$= C_{R_2}(\cos\alpha_m\cos\sigma_2 + \sin\alpha_m\sin\sigma_2)$$

On the basis of linear variation of force between tips, the initial condition for rotary instability is that

$$C_{\Delta_1} > C_{\Delta_2}$$

or

$$C_{\Delta_2} - C_{\Delta_1} < 0.$$

We may write

$$C_{\Delta_2} - C_{\Delta_1} = C_{R_2}(\cos\alpha_m\cos\sigma_2 + \sin\alpha_m\sin\sigma_2) - C_{R_1}(\cos\alpha_m\cos\sigma_1 - \sin\alpha_m\sin\sigma_1)$$

$$= \cos\alpha_m\,(C_{R_2}\cos\sigma_2 - C_{R_1}\cos\sigma_1) + \sin\alpha_m\,(C_{R_2}\sin\sigma_2 - C_{R_1}\sin\sigma_1).$$

Dividing both sides by $2\Delta\alpha$ we note that in the limit

$$\frac{C_{\Delta_2} - C_{\Delta_1}}{2\Delta\alpha} = \frac{d(C_\Delta)}{d\alpha}$$

$$\frac{C_{R_2}\cos\sigma_2 - C_{R_1}\cos\sigma_1}{2\Delta\alpha} = \frac{d(C_R\cos\sigma)}{d\alpha}$$

$$\frac{C_{R_2}\sin\sigma_2 - C_{R_1}\sin\sigma_1}{2\Delta\alpha} = \frac{d(C_R\sin\sigma)}{d\alpha}$$

and the criterion becomes

$$\frac{d(C_\Delta)}{d\alpha} = \cos\alpha_m\frac{d(C_R\cos\sigma)}{d\alpha} + \sin\alpha_m\frac{d(C_R\sin\sigma)}{d\alpha} < 0 \tag{7}$$

Figure 17 shows the variation of σ with angle of attack for the models tested. Since $\sigma < 10°$ the following approximations may be made, the criterion becoming

$$\cos \alpha_m \frac{d(C_R)}{d\alpha} + \sin \alpha_m \frac{d(C_R\sigma)}{d\alpha} < 0$$

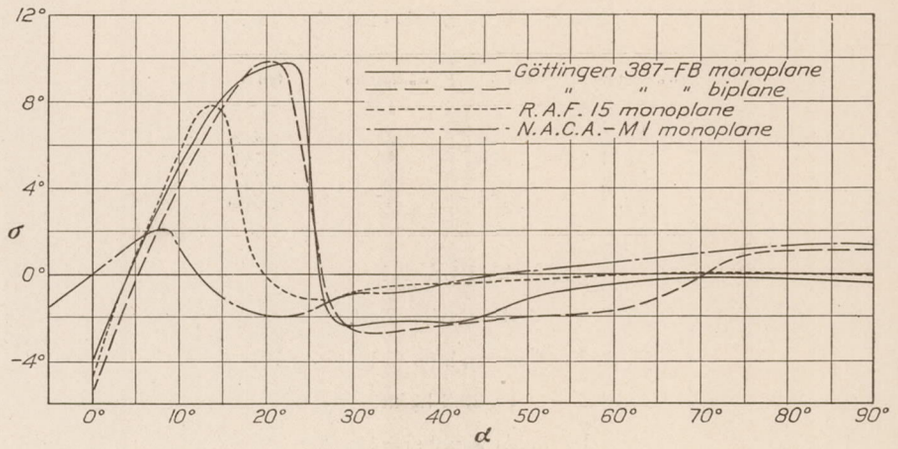

FIG. 17.—Curves of σ vs. α

Figure 15 shows that with the exception of the maximum negative values of $\frac{d(C_A)}{d\alpha}$ the second term of equation (7) is negligible and since $\cos \alpha_m$ is always positive in the first quadrant, our criterion becomes

$$\frac{d(C_R)}{d\alpha} < 0 \tag{8}$$

Glauert's criterion is

$$\frac{d(C_L)}{d\alpha} + C_D < 0$$

which is exact, but equation (8), in spite of its approximate nature, for all practical purposes, gives the same results.

TABLE I

Autorotation Test

Göttingen 387—FB biplane (5 by 30 inches)

$G/c = 1$, stagger $= 0$

$q = 20.2$ kg/m^2

Reynolds Number $= 155{,}000$

α_m degrees	tan ϕ	α_m degrees	tan ϕ
20	0. 373	47. 5	1. 125
22	. 417	50	1. 197
25	. 482	54. 3	1. 293
27. 5	. 528	59. 9	1. 382
30	. 593	61. 8	1. 373
32. 5	. 696	66. 7	1. 338
35	. 787	69. 2	1. 322
40	. 945	74. 7	1. 930
45	1. 063		

TABLE II

Autorotation Test

Göttingen 387—FB monoplane (5 by 30 inches)

q=20.2 kg/m²

Reynolds Number=153,000

α_m degrees	tan ϕ	α_m degrees	tan ϕ
17. 1	0. 319	25	0. 458
19. 5	. 376	30	. 503
20. 2	. 389	33. 5	. 526
22. 5	. 429	37	. 509

TABLE III

Autorotation Test

R. A. F. 15 monoplane (5 by 30 inches)

q=20.2 kg/m²

Reynolds Number=152,000

α_m degrees	tan ϕ	α_m degrees	tan ϕ
15	0. 152	31	0. 308
15. 4	. 161	32	. 214
17	. 228	32. 5	. 196
20. 2	. 307	33. 8	. 161
25	. 338	34. 1	. 147
30	. 341		

TABLE IV

Autorotation Test

N. A. C. A.–M1 monoplane (5 by 30 inches)

q=20.2 kg/m²

Reynolds Number=153,000

α_m degrees	tan ϕ	α_m degrees	tan ϕ
16	0. 078	22. 1	0. 236
16. 5	. 093	25	. 257
18. 1	. 152	28	. 238
20	. 208	28. 6	. 115

TABLE V

Force Test

Göttingen 387–FB biplane (5 by 30 inches)

$G/c=1$, stagger=0

$q=20.2$ kg/m²

Reynolds Number=156,000

α degrees	C_L	C_D	α degeees	C_L	C_D
−8	−0. 006	0. 046	30	0. 784	0. 509
−6	+. 100	. 030	35	. 766	. 598
−3	. 262	. 028	40	. 734	. 676
0	. 438	. 037	45	. 669	. 730
+3	. 620	. 051	50	. 596	. 769
6	. 798	. 072	55	. 505	. 788
9	. 958	. 098	60	. 415	. 776
12	1. 104	. 126	65	. 312	. 728
15	1. 236	. 160	70	. 226	. 634
18	1. 324	. 198	75	. 170	. 633
21	1. 365	. 244	80	. 128	. 656
24	1. 052	. 344	85	. 072	. 676
27	. 842	. 450	90	. 014	. 682

TABLE VI

Force Test

Göttingen 387–FB monoplane (5 by 30 inches)

$q=20.2$ kg/m²

Reynolds Number=155,000

α degrees	C_L	C_D	α degrees	C_L	C_D
−8	−0. 005	0. 052	30	0. 840	0. 538
−6	+. 127	. 030	32	. 876	. 602
−3	. 323	. 029	35	. 892	. 680
0	. 534	. 036	40	. 851	. 776
+3	. 744	. 050	45	. 811	. 854
6	. 948	. 070	50	. 751	. 941
9	1. 136	. 095	55	. 700	1. 028
12	1. 285	. 124	60	. 631	1. 124
15	1. 377	. 162	65	. 544	1. 195
18	1. 418	. 217	70	. 452	1. 270
21	1. 378	. 283	75	. 347	1. 328
24	1. 260	. 331	80	. 232	1. 336
25	1. 075	. 395	85	+. 113	1. 390
27	. 836	. 461	90	−. 009	1. 389

TABLE VII

Force Test

R. A. F. 15 monoplane (5 by 30 inches)

q=20.2 kg/m²

Reynolds Number=155,000

α degrees	C_L	C_D	α degrees	C_L	C_D
−2	−0. 015	0. 016	30	0. 866	0. 523
0	+. 163	. 015	35	. 938	. 679
+3	. 383	. 021	40	. 908	. 786
6	. 597	. 035	45	. 834	. 854
9	. 810	. 055	50	. 760	. 929
12	. 981	. 081	55	. 703	1. 016
13	1. 011	. 094	60	. 637	1. 111
15	1. 025	. 138	65	. 558	1. 205
18	. 907	. 279	70	. 463	1. 276
21	. 804	. 324	75	. 353	1. 335
23	. 789	. 355	80	. 241	1. 382
25	. 789	. 391	85	+. 119	1. 420
27	. 804	. 438	90	−. 008	1. 409

TABLE VIII

Force Test

N. A. C. A.–M1 monoplane (5 by 30 inches)

q=20.2 kg/m²

Reynolds Number=155,000

α degrees	C_L	C_D	α degrees	C_L	C_D
0	−0. 006	0. 011	40	0. 863	0. 746
3	+. 216	. 015	45	. 802	. 816
6	. 422	. 032	50	. 725	. 881
9	. 619	. 081	55	. 680	. 970
12	. 717	. 159	60	. 619	1. 066
15	. 694	. 207	65	. 546	1. 153
18	. 680	. 248	70	. 463	1. 233
21	. 695	. 298	75	. 369	1. 296
25	. 735	. 374	80	. 266	1. 345
30	. 837	. 508	85	. 155	1. 375
35	. 883	. 648	90	. 031	1. 377

ADDITIONAL COPIES
OF THIS PUBLICATION MAY BE PROCURED FROM
THE SUPERINTENDENT OF DOCUMENTS
U.S. GOVERNMENT PRINTING OFFICE
WASHINGTON, D. C.
AT
10 CENTS PER COPY

▽

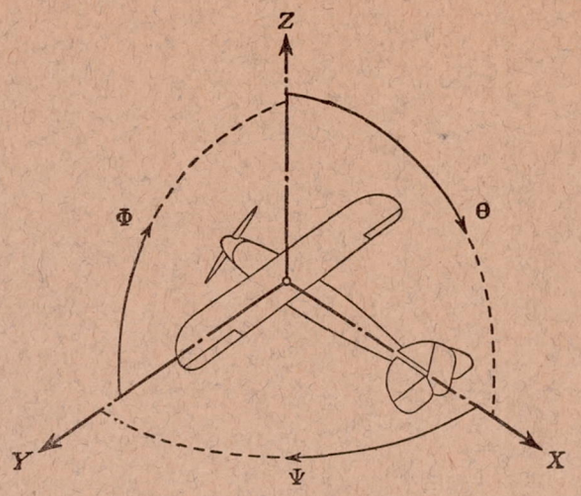

Positive directions of axes and angles (forces and moments) are shown by arrows

Axis		Force (parallel to axis) symbol	Moment about axis			Angle		Velocities	
Designation	Symbol		Designation	Symbol	Positive direction	Designation	Symbol	Linear (component along axis)	Angular
Longitudinal	X	X	rolling	L	$Y \longrightarrow Z$	roll	Φ	u	p
Lateral	Y	Y	pitching	M	$Z \longrightarrow X$	pitch	Θ	v	q
Normal	Z	Z	yawing	N	$X \longrightarrow Y$	yaw	Ψ	w	r

Absolute coefficients of moment

$$C_L = \frac{L}{qbS} \quad C_M = \frac{M}{qcS} \quad C_N = \frac{N}{qfS}$$

Angle of set of control surface (relative to neutral position), δ. (Indicate surface by proper subscript.)

4. PROPELLER SYMBOLS

D, Diameter.
p_e, Effective pitch
p_g, Mean geometric pitch.
p_s, Standard pitch.
p_v, Zero thrust.
p_a, Zero torque.
p/D, Pitch ratio.
V', Inflow velocity.
V_s, Slip stream velocity.

T, Thrust.
Q, Torque.
P, Power.
(If "coefficients" are introduced all units used must be consistent.)
η, Efficiency $= T\,V/P$.
n, Revolutions per sec., r. p. s.
N, Revolutions per minute., R. P. M.
Φ, Effective helix angle $= \tan^{-1}\left(\frac{V}{2\pi rn}\right)$

5. NUMERICAL RELATIONS

1 HP = 76.04 kg/m/sec. = 550 lb./ft./sec.
1 kg/m/sec. = 0.01315 HP.
1 mi./hr. = 0.44704 m/sec.
1 m/sec. = 2.23693 mi./hr.

1 lb. = 0.4535924277 kg.
1 kg = 2.2046224 lb.
1 mi. = 1609.35 m = 5280 ft.
1 m = 3.2808333 ft.